

Earthquake risk assessment of concrete gravity dam by cumulative absolute velocity and response surface methodology

Anh-Tuan Cao¹, Tahmina Tasnim Nahar^{1,2}, Dookie Kim*¹ and Byounghan Choi³

¹Department of Civil Engineering, Kunsan National University, Republic of Korea

²Department of Civil Engineering, Pabna University of Science and Technology, Bangladesh

³Rural Research Institute, 870, Haean-ro Sangnok-gu, Ansan-si Gyeonggi-do, 15634, Republic of Korea

(Received August 13, 2018, Revised August 13, 2019, Accepted October 15, 2019)

Abstract. The concrete gravity dam is one of the most important parts of the nation's infrastructure. Besides the benefits, the dam also has some potentially catastrophic disasters related to the life of citizens directly. During the lifetime of service, some degradations in a dam may occur as consequences of operating conditions, environmental aspects and deterioration in materials from natural causes, especially from dynamic loads. Cumulative Absolute Velocity (CAV) plays a key role to assess the operational condition of a structure under seismic hazard. In previous researches, CAV is normally used in Nuclear Power Plant (NPP) fields, but there are no particular criteria or studies that have been made on dam structure. This paper presents a method to calculate the limitation of CAV for the Bohyeonsan Dam in Korea, where the critical Peak Ground Acceleration (PGA) is estimated from twelve sets of selected earthquakes based on High Confidence of Low Probability of Failure (HCLPF). HCLPF point denotes 5% damage probability with 95% confidence level in the fragility curve, and the corresponding PGA expresses the crucial acceleration of this dam. For determining the status of the dam, a 2D finite element model is simulated by ABAQUS. At first, the dam's parameters are optimized by the Minitab tool using the method of Central Composite Design (CCD) for increasing model reliability. Then the Response Surface Methodology (RSM) is used for updating the model and the optimization is implemented from the selected model parameters. Finally, the recorded response of the concrete gravity dam is compared against the results obtained from solving the numerical model for identifying the physical condition of the structure.

Keywords: cumulative absolute velocity; fragility curve; response surface methodology; system identification; structural health monitoring; risk analysis

1. Introduction

Earthquake risk assessment became an important affair nowadays to give the decision regarding the operational condition of any structure. All over the world, the concrete gravity dam acts as a vital civil engineering part because it has different structural characteristics than other structures. In Korea, there are several dams are designed in seismic prone areas to resist the unpredictable earthquakes and their design life is more than fifty years. Although the dams are constructed under the seismic consideration, the deterioration in a concrete gravity dam generally occurred due to the consequences of operating conditions, environmental aspects, and degradation in materials from natural causes.

This paper presents the seismic analysis of the Bohyeonsan Dam in Korea. For predicting the present operational condition, the Cumulative Absolute Velocity (CAV) is an important ground motion intensity measurement (IM). Based on predicting CAV standard, Du and Wang (2013) developed a model using Next Generation Attenuation (NGA) strong database, where the proposed

model employs only four parameters and has a simple functional form. Kramer and Mitchell (2006) mentioned the CAV₅, a new measurement standard, which shows the excess pore pressure generation in potentially liquefiable soils is considerably more closely related to CAV₅ than to other intensity measures, including peak acceleration and arias intensity. Another study about the site's effects in the Taipei areas of Taiwan based on CAV amplification was investigated, where more than 1200 strong motions were gathered from the database (Wang *et al.* 2018). The analytical results indicated that strong site's effects should exist in western Taipei and in the locations close to the rims of the Taipei Basin. Moreover, Reed and Kassawara (1990) provided a criterion for a nuclear power plant, and this criterion requires exceedance of both response spectrum parameter and second damage parameter, referred to the CAV. The unfiltered arias intensity and CAV give a good correlation with the macroseismic information (Cabanas *et al.* 1997). Safety assessment against the seismic hazard of the NPP is a common issue, Katona (2013) established criterion in terms of CAV for determination of fatigue failure considering the cyclic loading and the degradation. Furthermore, in a technical report, Hardy *et al.* (2006) made a CAV model for computation probabilistic seismic hazard of NPP based upon the review of CEUS and WUS data with considering the functions of uniform duration, magnitude, PGA and wave velocity. Campbell and Bozorgnia (2010,

*Corresponding author, Professor
E-mail: kim2kie@kunsan.ac.kr

2011) mentioned an empirical equation of EPRI (1988) by using the strong motion database for the horizontal component of CAV. Besides that, EPRI (1991) also established another equation called standardized CAV for giving the criteria to stop or continue the structural operation (O'Hara and Jacobson 1991). However, there is no strategy has been studied on CAV limitation for the concrete gravity dam.

The Response Surface Methodology (RSM) is used for the system identification (SI) of the Bohyeonsan concrete dam, where parameters are selected by using the Central Composite Design (CCD) method. Kartal *et al.* (2011) used the RSM for selecting the parameters in a concrete-faced rockfill (CFR) dam because of its various uncertainties in the body. For solving these uncertainties such as the mechanical properties of materials, geometric properties, load magnitude, and distribution, etc., RSM is a helpful tool (Abu-Odeh and Jones 1998, Chávez-Valencia *et al.* 2007, Lee and Lin 2003).

Ghanaat *et al.* (2015) presented a methodology for developing seismic fragility of concrete gravity dams, in which the lognormal distribution reasonably well, it provides the median seismic fragility, including randomness and uncertainty for the base sliding and pier failure. In addition, Padgett and DesRoches (2008) studied the fragility curve for a multi-span continuous concrete girder bridge, which indicates the retrofiting dimension according to the damage probability. The damage level evaluation of real-time and the optimization of the required seismic performance level on cost-benefit analysis is explained by Ichii (2004). In another study, Lin and Adams (2008) have developed a probabilistic method for seismic ranking of 133 hydropower dams in Canada, where the fragility curves were associated to the dam type and the construction period. The fragility curve including the spatial variation of the angle of friction, reveals a slight effect on the curve for vulnerability assessment of the dam and is mainly critical during severe damage (Bernier *et al.* 2015). Beilic *et al.* (2017) have proposed a seismic fragility model for Italian RC precast buildings, where the risk assessment was compared to two building topologies; these curves were derived using both nonlinear static and dynamic analysis. Furthermore, Mosleh *et al.* (2016) determined the probabilistic fragility analysis for a bridge would reach or exceed the structural capacity by considering PGA and Acceleration Spectrum Intensity (ASI). In this research, uncertainty analysis for the fragility is estimated by determining the High Confidence Low Probability of Failure (HCLPF) (Kim *et al.* 2011). In seismic risk assessment for the NPP, the capacity of a secondary system is measured in terms of resistance to undesirable response or failure, which is characterized by the HCLPF point (Huang *et al.* 2006). Borgonovo *et al.* (2013) described that the HCLPF point is used to determine the seismic risk analysis for civil engineers as a conservative estimation of components or structure's capacity.

The purpose of this study is to assess the operational condition of the Bohyeonsan Dam after withstanding the Pohang earthquake. According to previous researches, Du and Wang (2013) mentioned that the CAV has higher predictability than other intensity measures such as PGA.

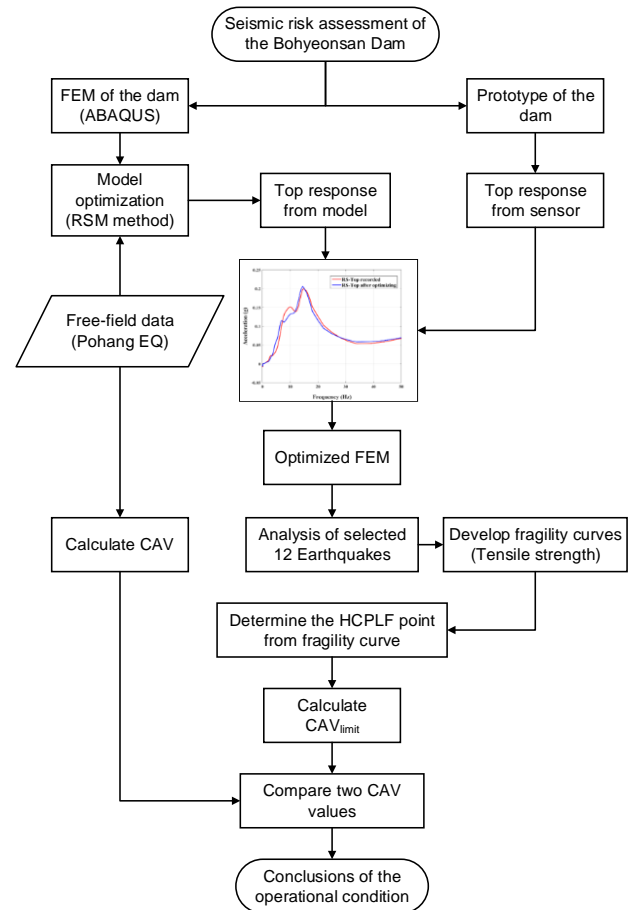


Fig. 1 The Bohyeonsan Dam risk assessment process

For estimating the dam's CAV limitation, a set of twelve earthquakes in Korea provided by K-water organization is used to develop the fragility curves using the Incremental Dynamic Analysis (IDA) method mentioned by Baker (2015). A 2D finite element model (FEM) has been adopted by using ABAQUS. Hoseini Vaez and Arefzade (2017) used 4-node quadrilateral elements of plane stress with reduced integration is denoted as CPS4R in the numerical model. There were two sensors installed on the top and the bottom of the dam to record the acceleration response, and the section corresponding to the location of the sensors is selected for numerical simulation. The Pohang earthquake recorded data is applied as the input ground motion in the model to evaluate the response surface of the dam. To be more understandable, the following flowchart expresses the glance of this paper.

2. Specification of the Bohyeonsan Dam

The Bohyeonsan Dam is located in the upper stream of Gohyeoncheon, which is the second tributary of the Kumho river. The total dam crest length is 250 m, whereas the maximum height is 57 m. Figs. 2(a) and (b) express the location of the sensors to get earthquake measurement data and the overview of the structure, respectively. In addition, the following Tables 1-2-3 present the specification of this dam. Considering the convenience of transportation and



(a) The sensor's location



(b) The construction site (K-water 2018)

Fig. 2 The three-dimensional view of the Bohyeonsan Dam

Table 1 Specification of the Bohyeonsan Dam

Specification	SL	Structure name
$H = 57\text{ m}, L = 250\text{ m}$	6	Sub dam
$H = 15.3\text{ m}$	7	Small hydropower plant
17 Passengers	8	Upstream tide
$B\ 2.0 \times H\ 2.5\text{ m}$	9	Garbage collection
$m\ B\ 6.0 \times L\ 9.0 \times H\ 5.0\text{ m}$	10	Flow wall

Table 2 Design water level

Division	Upper water level (m)	Downstream level (m)
Highest water level	EL. 240.00	EL. 188.28
Planning flood level	EL. 238.50	EL. 185.11
Constant water level	EL. 236.00	-
Low water level	EL. 208.00	-

installation of heavy equipment during the construction, the dam floor has two lanes for vehicle traffic as the access to the road and security. Therefore, the width of the paraplegic parapet and auxiliary pedestrian bridge is 8.5 m, including the walkway, and the width of the pedestrian bridge is 7 m considering the interference of the waterway. A gallery was installed inside the dam so that construction and maintenance can be done after completion.

The Bohyeonsan Dam significantly is used for the controlling of reservoir water. The whole storage capacity of the reservoir is $22.10 \times 10^6\text{ m}^3$ and the construction of the dam was completed in 2014. Two rows PVC panels were installed to prevent lateral shrinkage and leakage of joints and leakage. The detailing dimensions of the selected overflow section of the Bohyeonsan Dam are determined and described in Fig. 3.

Table 3 Concrete materials properties

Material properties	Inside the dam	Outside the dam
Design criteria of compressive strength (MPa)	12	18
Young's modulus (MPa)	13767	16861
The tensile strength (MPa)	1.3	1.6
Poisson's ratio	0.18	0.18
Density (kg/m^3)	2300	2300
Compressive strength estimate coefficient	a	b
	d	c
	16.2	16.2
	0.82	0.82
	1.00	1.00

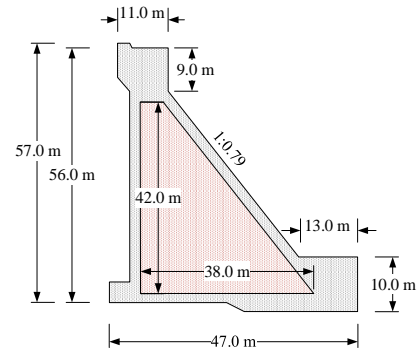


Fig. 3 Detailing dimensions of the selected section

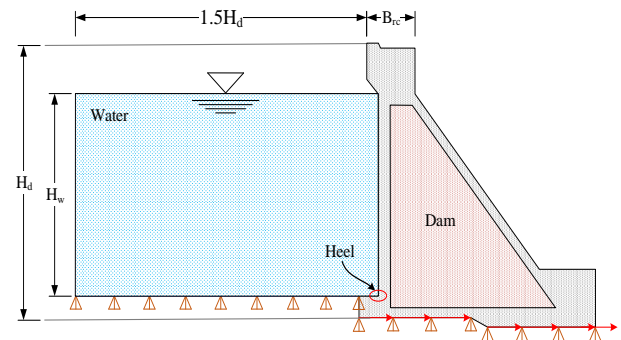


Fig. 4 Geometry of the Bohyeonsan concrete dam

3. Finite element analysis and model verification

3.1 Finite element model

For system identification to find out the parameters of this dam, a 2D finite element model is simulated by ABAQUS. The most critical section has been chosen according to the acceleration and stress output of the model analysis. Fig. 3 describes the selected cross-section with dimensions, and Fig. 4 shows the geometry of the Bohyeonsan concrete gravity dam.

From the geometry, it can be seen that this dam is built using two kinds of concrete with different elastic modulus. The element type CPS4R (4-node bilinear plane stressed quadrilateral) is used in the numerical model. Water pressure is included in the PohangEQ step, in which the height of the equivalent water level is $H_w = 42\text{ m}$ from the heel. During the optimization of the model, the free field data of the Pohang earthquake is considered as the input ground motion. According to Mridha and Maity (2014), the

first stage to get the natural frequency is essential for structural analysis.

3.2 System identification using Response Surface Methodology (RSM)

Many methods have been used for system identification in previous studies; it is apparently undeniable that Response Spectral (RS) obtained from accelerometers reflects exactly the dynamic response of the structure. Moreover, to enhance the accuracy of the structural health monitoring, multi-objective optimization using RSM is applied in this section. Myers *et al.* (2016) concluded that the response surface methodology is a collection of mathematical models, which are convenient for analyzing and building an empirical model. Depending on the set of tests, RSM estimates the relationship between several variables (v) and responses (r) of the structure by Eq. (1).

$$r = f(v_1, v_2, \dots, v_n) + u \tag{1}$$

where u describes the error observed (offset term) in the response r and $f(v_1, v_2, \dots, v_k)$ deputizes the response of the structure due to the sets of input variables. By using an interesting range of parameters, the optimization of response can be obtained from several independent variables. First-order and second-order polynomial equations are commonly used for RSM, which are expressed as Eqs. (2)-(3).

First-order:

$$r = \beta_0 + \sum_{i=1}^n \beta_i v_i + \sum_{i,j=1}^n \beta_{ij} v_i v_j + u \tag{2}$$

Second-order:

$$r = \beta_0 + \sum_{i=1}^n \beta_i v_i + \sum_{i=1}^n \beta_i v_i^2 + \sum_{i,j=1}^n \beta_{ij} v_i v_j + u \tag{3}$$

where r is the predicted response and β is the estimated partial regression coefficient of noise; v_i is the coded factor ($i, j = 1, 2, 3, \dots, n$) and u is the offset term. Although the polynomial Eq. (3) can be used with greater order, it is sufficient for solving the engineering problems with the second order. In this study, the CCD method is used for identifying the structural parameters.

Central Composite Design (CCD)

For the optimization of responses (output variables), the CCD is a design experiment tool (Sadhukhan *et al.* 2016). The CCD is effective to predict the output by using an equation based on central and axial points with factorial design. The total number of experiments is calculated by the following equation

$$S = 2^n + 2n + c_p \tag{4}$$

where n is the number of factor and c_p is the number of center-point. In this study, two factors are used as the proportion of Young's modulus and density, while the

Table 4 Experimental region of material parameters

Factors	Interest region		
	Low	Center	High
Proportion of Young's modulus (α)	0.66364	1	1.33636
Density (tone/m ³)	2.20000	2.325	2.45000

Table 5 The analysis points and corresponding structural responses

Run order	Analysis point		Structural responses	
	E (α)	ρ	F_1	F_2
1	0.66364	2.32500	18.0	0.23795
2	1.00000	2.32500	14.5	0.18989
3	1.20000	2.45000	14.5	0.17441
4	0.80000	2.45000	18.0	0.20087
5	0.80000	2.20000	14.0	0.21748
6	1.00000	2.11478	14.5	0.21106
7	1.33636	2.32500	14.0	0.17920
8	1.00000	2.53522	14.0	0.17622
9	1.20000	2.20000	14.0	0.19784

Table 6 Equations for predicting frequency and peak acceleration values

Cases	Object function	Prediction equations
1	PA_F	$0.926 - 0.248\alpha - 0.413\rho + 0.1655\alpha^2 + 0.086\rho^2 - 0.068\alpha \times \rho$
2	FA_F	$-92 + 50.4\alpha + 69\rho + 12.9\alpha^2 - 6.7\rho^2 - 35\alpha \times \rho$

acceleration at the top of the dam under the Pohang earthquake is inspected as the structural response. The top acceleration and frequency response values have been considered as objective functions and the Eqs. (5)-(6) explain their meaning

$$F_1 = (FA_F) \tag{5}$$

$$F_2 = (PA_F) \tag{6}$$

where (PA_F) ($F = 1, 2, \dots, k$) is the peak value of acceleration on the frequency domain and (FA_F) ($F = 1, 2, \dots, k$) is the value of frequency corresponding to the peak acceleration. Using Eq. (4), CCD creates a total of 9 experimental points, including 4 factorial points, 4 axial points and 1 center point, which are generated randomly from the interest region of the proportion of Young's modulus (α) and density (ρ) (Hussan *et al.* 2018). The interest region is shown in Table 4.

In order to carry out the structural optimization, the acceleration amplitude and frequency values are chosen as objective functions to minimize the difference between the numerical model and the real structure. All of the optimization cases are designed by using Minitab (2018) tools. Table 5 enumerates the analysis cases of the Bohyeonsan Dam under the Pohang earthquake, and Table 6 shows the equations for predicting the frequency value and peak acceleration.

To make it more understandable, the surface plot function is conducted to show the three-dimensional view

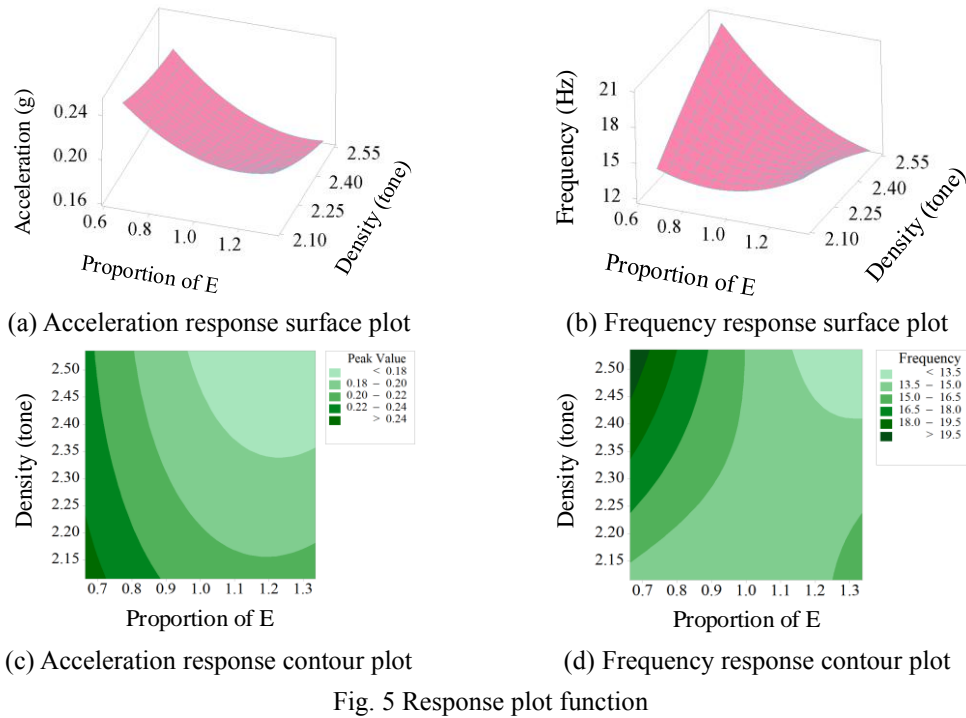


Fig. 5 Response plot function

Table 7 Similarity comparison of RS

		Before optimizing	After optimizing
Similar (%)	Acceleration	92.8	97.3
	Frequency	93.3	96.7

of response due to changing the factors. Fig. 5 portrays the structural response, which is plotted along with the two factors of concrete material. Besides that, the structural optimization using the response optimizer function based on RSM is applied herein. For optimization cases of dam's parameters, the peak acceleration and frequency obtained from sensors are considered as target objects. Fig. 6 expresses the response of the structure, which mainly based on the target value set up to find out the enrich results. The optimum proportion of Young's modulus (α) and density (ρ) after optimizing is 0.787 and 2.32 (tone/m³), respectively.

Figs. 6 (a) and (b) show the response spectrum at the top of the dam before and after optimizing, the difference between the peak acceleration and frequency is decreased when compared with the recorded data. The percentage of similarities of Response Spectrums (RS) are shown in Table 7 for better understanding.

From the above analysis, it indicates that that the response of the dam after using RSM is not exactly matched because of many uncertain factors, but from Fig. 6(b) and from the percentage value after optimizing we can say that these results are acceptable.

4. Fragility analysis

A fragility curve expresses the probability of failure of a structure corresponding to the input motion intensity measure, such as the PGA (Tran *et al.* 2019). Fragility

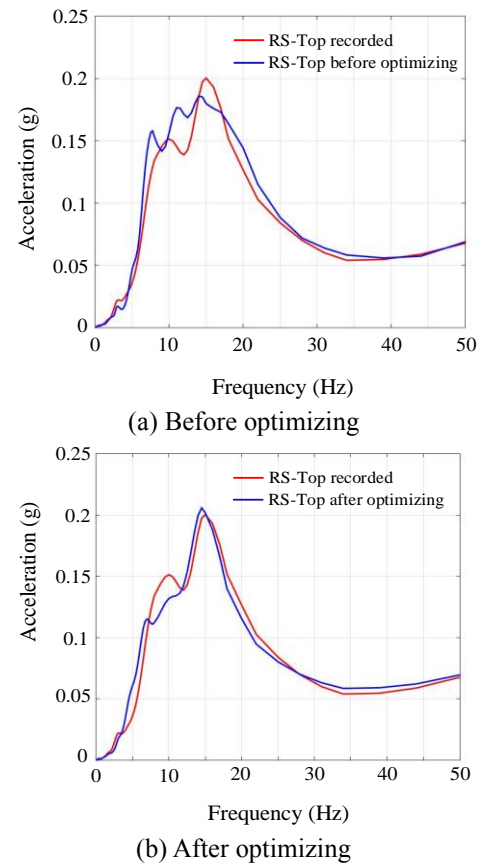


Fig. 6 Response spectrum on the top of the dam

curves also become very popular for assessing the seismic vulnerability of civil engineering structures and it is one of the best current practices. Vamvatsikos and Cornell (2002) studied about IDA, which involves a series of structural dynamic analyses under a set of ground motion records.

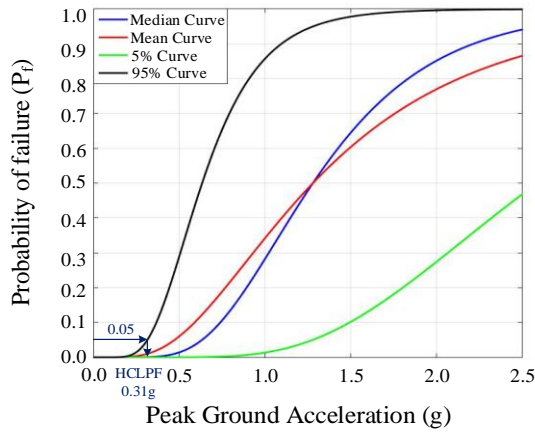


Fig. 7 Fragility curves of the Bohyeonsan Dam

Each recorded data is scaled into several intensity levels to cover the whole range from elastic to collapse of the structure. Particularly, the goal of the analysis is to record the damage state of the dam, which is measured by an engineering demand parameter. In this study, the tensile strength of concrete material is considered as the limit-states of a structure. According to Ibarra and Krawinkler (2005), the fragility curve is calculated from data sets by taking logarithms of each ground motion's IM value corresponding to the onset of collapse, the mean and standard deviation values are calculated by Eqs. (7)-(8).

$$\ln\theta = \frac{1}{n} \sum_{i=1}^n \ln IM_i \quad (7)$$

$$\beta = \sqrt{\frac{1}{n-1} \sum_{i=1}^n (\ln(IM_i/\theta))^2} \quad (8)$$

The exceedance in the PGA and the probability of failure are analyzed by applying twelve sets of earthquakes in Korea as input ground motions with various IM levels. After carrying out the fragility analysis, the fragility curves of the dam are shown in Fig. 7, which reflects the vulnerability of the structure. A new idea is proposed throughout this study is the estimation of CAV_{limit} for dam structure based on PGA value, which comes from the HCLPF point. Reed and Kennedy (1994) described the HCLPF capacity is defined to be the 95% confidence of a 5% probability of exceedance. Sen (2018) mentioned that the 5% probability of failure is common in all civil engineering structures to check the safety against earthquakes.

Fig. 7 indicates that the HCLPF point for the Bohyeonsan Dam is defined from the 95% confidence fragility curve with a 5% probability of failure. The failure starts from 5% corresponding to PGA of 0.31 g and leads to the total collapse of the dam at the level of more than 2.5 g. The major purpose of developing fragility curve for the structural model is to reflect the vulnerability of structural behavior. From the acceleration value of the HCLPF point, the cumulative absolute velocity analysis is conducted. Firstly, all of the selected earthquakes are scaled so that the

peak ground acceleration is 0.31 g. Then, the capacity of CAV_{limit} is calculated and chosen conservatively for checking the operational condition of the structure. The detailed process is explained clearly in the next sections.

5. Cumulative absolute velocity (CAV) and standardized CAV

Based on the CAV threshold value, the dam operators can give the decision whether a dam must be shut down after an earthquake event or not. According to Campbell and Bozorgnia (2011), CAV is defined as the integral of the absolute acceleration values in the time domain, which is represented mathematically by the Eq. (9)

$$CAV = \int_0^{t_{\max}} |a(t)| dt \quad (9)$$

where $a(t)$ is acceleration value, t is time, and t_{\max} is the total duration of the time series. Fig. 8 illustrates the acceleration response in the time domain and the corresponding value of CAV (Campbell and Bozorgnia 2010). In this figure, CAV is the summation of the hatched areas. Obviously, the value of CAV increases with time until reaching the maximum value at t_{\max} . Therefore, it is not skeptical to say that CAV includes total effects of the whole ground motion, and the Electrical Power Research Institute (EPRI 1988) detected that it is the best ground motion parameter. As reported by Hardy *et al.* (2006), EPRI introduced a standardized version of CAV_{STD} , which rejects the contribution of low-amplitude and non-damaging ground motions from contributing to probabilistic seismic hazard analysis. The mathematical explanation of CAV_{STD} is described in Eqs. (10)-(11).

$$CAV_{STD} = \sum_{i=1}^N \left(H(PGA_i - \ddot{u}_{\min}) \int_{i+1}^i |a(t)| dt \right) \quad (10)$$

$$H(\delta) = \begin{cases} 0 & \delta < 0 \\ 1 & \delta \geq 0 \end{cases} \quad (11)$$

where N is the number of non-overlapping for one-second time intervals, PGA_i is the peak ground acceleration (g) in i_{th} time step, \ddot{u}_{\min} is an acceleration threshold (user-defined, but usually taken as 0.025 g) to neglect low-amplitude motions contributing to the summation, $H(\delta)$ is the Heaviside step function.

The small-amplitude accelerations usually do not cause significant consequences on structural damages, so several versions of CAV are suggested to exclude these small-amplitude values. For instance, the version of the standardized CAV method (CAV_{STD}) only calculates for the 1-sec time interval range, which has at least one peak acceleration value greater than the threshold value of 0.025 g. Kramer and Mitchell (2006) mentioned another variant CAV namely CAV_5 , which includes the acceleration values greater than the threshold value of 5 cm/sec². However, the exclusion of low-amplitude acceleration, especially values near the acceleration threshold leads to declining stability in predicting these intensity measures (Campbell and Bozorgnia 2010). Collaborate with this reason and almost

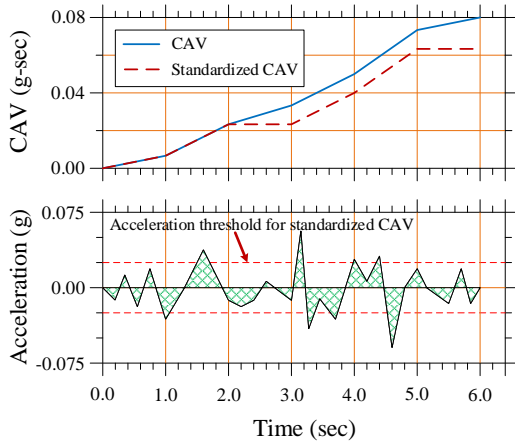
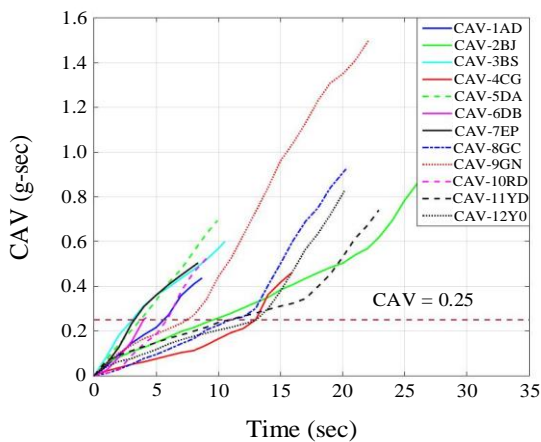
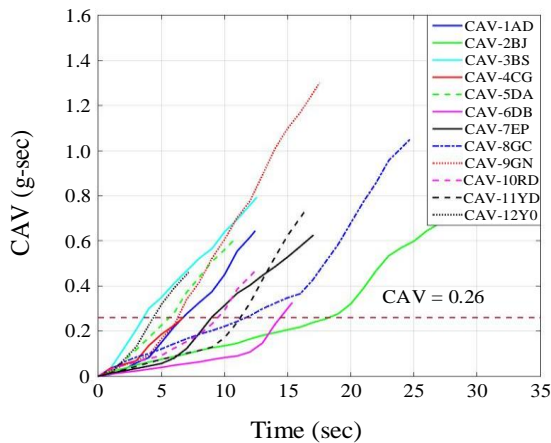


Fig. 8 Illustration of the CAV definition



(a) North-South direction



(b) East-West direction

Fig. 9 CAV calculation corresponding to 12 selected earthquakes in Korea

the acceleration values of the Pohang earthquake data are smaller than the acceleration threshold (0.025 g), thus, the only CAV method is used in this paper to increase the reliability.

6. Calculating CAV limitation and checking the operational condition of the dam

Table 8 CAV values of earthquake data sets in Korea

Earthquake	1AD	2BJ	3BS	4CG	5DA	6DB	7EP	8GC	9GN	10RD	11YD	12Y0
CAV-N	0.44	1.20	0.60	0.46	0.69	0.25	0.50	0.93	1.50	0.54	0.74	0.83
CAV-E	0.64	0.69	0.79	0.26	0.61	0.33	0.63	1.05	1.30	0.47	0.88	0.46

The CAV concept is the best single parameter for specifying the damage threshold of earthquake impacts. Fig. 7 presents the boundary of fragility curves and from the curve of 95% confidence level, the PGA 0.31 g of HCLPF point presents 5% probability of failure. In order to calculate the limitation of CAV for the dam, all of the earthquakes in data sets are scaled, analyzed with this PGA, and these results are presented in Fig. 9. From this figure, the capacity of CAV_{limit} is estimated by comparing the analysis of twelve earthquakes with two horizontal components. According to Hardy *et al.* (2006), the CAV values are defined for each free-field record and selected conservatively. In this study, Eq. (9) is applied for each earthquake in data sets and the effective duration of the time interval between 5% and 75% of arias intensity is used. The limitation is chosen as the lowest CAV value from CAV analysis. Result in, the minimum CAV value of 0.25 g is obtained from earthquake 6DB in the North-South direction. The summary of CAV values corresponding with each earthquake is enumerated in Table 8.

In the North-South (N-S) direction, the minimum CAV value is 0.25 g-sec from earthquake 6DB, whereas, in the East-West (E-W) direction, the obtained minimum CAV value is 0.26 g-sec for earthquake 4CG. Therefore, it can be said that the value of the CAV_{limit} of the Bohyeonsan Dam is 0.25 g-sec. The CAV check for any earthquake is exceeded if any one of the two horizontal components from the free-field ground motion is greater than 0.25 g-sec. Campbell and Bozorgnia (2010) explained that in the case of exceeding CAV_{limit} value, the Operating Basis Earthquake (OBE) is surpassed and plant shutdown is required.

After getting the CAV_{limit} value of the Bohyeonsan Dam, the cumulative absolute velocity inspection is conducted for free-field data sets of the Pohang earthquake. The high predictability of the CAV insures for using a simple functional form in checking the uncertainty in seismic hazard analysis. Besides that, this simplified method would have a significant advantage in situations where the ground-motion parameters for a sophisticated model are unknown or highly ambiguous.

The CAV calculation for the Pohang earthquake in two horizontal components is shown in Figs. 10-11, in which the maximum CAV value of 0.063g-sec is obtained from the East-West direction. Comparing with the dam capacity of CAV_{limit} (0.25g-sec), it can be said that the operational condition of the Bohyeonsan Dam is not affected after withstanding the Pohang earthquake.

7. Conclusions

Conducting the post-earthquake inspection of the structure becomes a financial burden for the governments. Therefore, proposing a time-saving and cost-effective

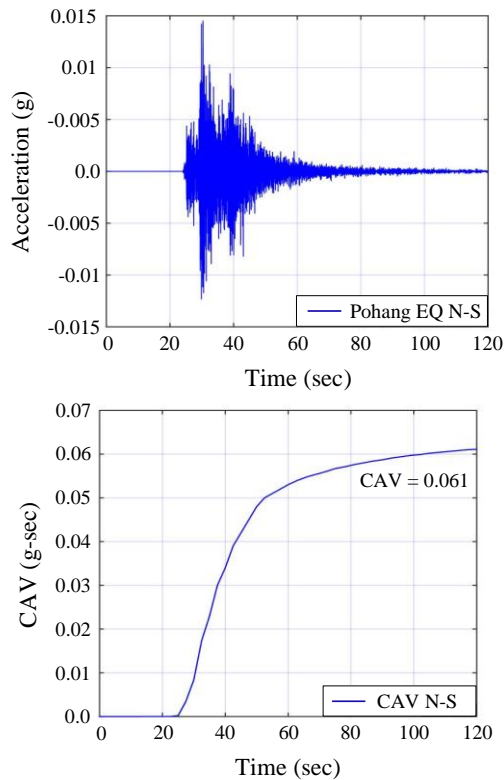


Fig. 10 CAV diagram in the N-S direction of the Pohang earthquake

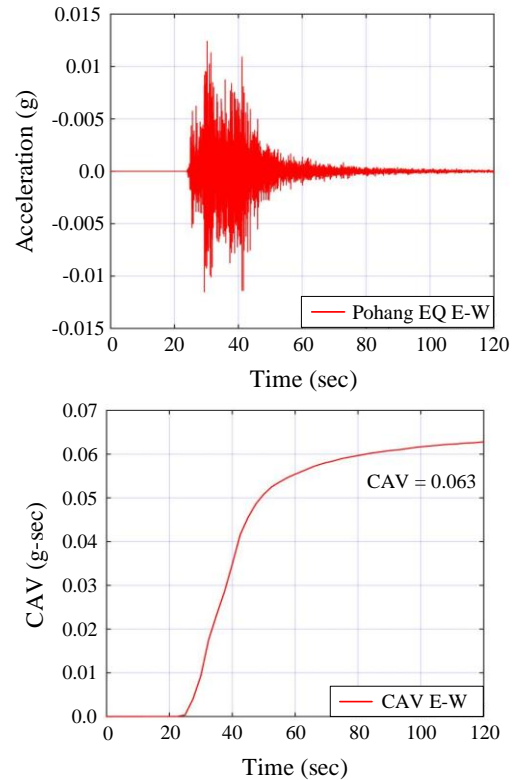


Fig. 11 CAV diagram in the E-W direction of the Pohang earthquake

method for making the preliminary evaluation by using the recorded data from sensors is the motivation of this study. The applicability of this method is the most important feature, based on the seismic risk assessment process for the Bohyeonsan Dam, the operators can apply for various structures in Korea. In addition, the user can alter flexibly the methods in each step to increase the accuracy.

During the lifetime of service, the characteristic of the structural material may be degradative by the impacts of uncertain issues such as seismic effects, chemo-mechanical phenomenon, etc. Predicting accurately the physical condition of the structure is a significant role in structural health monitoring. In order to improve the reliability of the numerical model, RSM is used to calibrate the acceleration output data. As the effects of the surrounding environmental condition of the dam, Young's modulus of elasticity is decreased by 21% whereas the density is increased by 0.87% more than the initial values. This phenomenon can be explained because the concrete continuously interacts with water during the service time, thus, the material properties are attenuate due to calcium leaching, mechanical damage, absorb water, etc. From the results of cumulative absolute velocity and fragility analysis, this study concludes that the operational condition of the Bohyeonsan Dam is not affected after withstanding the Pohang earthquake.

For the future research of this study, the inspection and prediction for the seismic vulnerability of dam structures in Korea at a specific coordinate should be considered. In addition, the soil-structure interaction (SSI) and fluid effects can be applied to improve the accuracy of the numerical model.

Acknowledgment

This research was supported by a grant (2017-MOIS31-002) from Fundamental Technology Development Program for Extreme Disaster Response funded by the Korean Ministry of Interior and Safety (MOIS).

References

- Abu-Odeh, A.Y. and Jones, H.L. (1998), "Optimum design of composite plates using response surface method", *Compos. Struct.*, **43**(3), 233-242. [https://doi.org/10.1016/S0263-8223\(98\)00109-3](https://doi.org/10.1016/S0263-8223(98)00109-3).
- Baker, J.W. (2015), "Efficient analytical fragility function fitting using dynamic structural analysis", *Earthq. Spectra*, **31**(1), 579-599. <https://doi.org/10.1193/021113EQS025M>.
- Beilic, D., Casotto, C., Nascimbene, R., Cicola, D. and Rodrigues, D. (2017), "Seismic fragility curves of single storey RC precast structures by comparing different Italian codes", *Earthq. Struct.*, **12**(3), 359-374. <https://doi.org/10.12989/eas.2017.12.3.000>.
- Bernier, C., Padgett, J.E., Proulx, J. and Paultre, P. (2015), "Seismic fragility of concrete gravity dams with spatial variation of angle of friction: case study", *J. Struct. Eng.*, **142**(5), 05015002. [https://doi.org/10.1061/\(ASCE\)ST.1943-541X.0001441](https://doi.org/10.1061/(ASCE)ST.1943-541X.0001441).
- Borgonovo, E., Zentner, I., Pellegrini, A., Tarantola, S. and de Rocquigny, E. (2013), "On the importance of uncertain factors in seismic fragility assessment", *Reliab. Eng. Syst. Saf.*, **109**, 66-76. <https://doi.org/10.1016/j.res.2012.08.007>.
- Cabanas, L., Benito, B. and Herráiz, M. (1997), "An approach to the measurement of the potential structural damage of earthquake ground motions", *Earthq. Eng. Struct. Dyn.*, **26**(1),

- 79-92. [https://doi.org/10.1002/\(SICI\)1096-9845\(199701\)26:1<79::AID-EQE624>3.0.CO;2-Y](https://doi.org/10.1002/(SICI)1096-9845(199701)26:1<79::AID-EQE624>3.0.CO;2-Y).
- Campbell, K.W. and Bozorgnia, Y. (2010), "A ground motion prediction equation for the horizontal component of cumulative absolute velocity (CAV) based on the PEER-NGA strong motion database", *Earthq. Spectra*, **26**(3), 635-650. <https://doi.org/10.1193/1.3457158>.
- Campbell, K.W. and Bozorgnia, Y. (2010), "Analysis of Cumulative Absolute Velocity (CAV) and JMA Instrumental Seismic Intensity (IJMA) using the PEER-NGA strong motion database", Pacific Earthquake Engineering Center, University of California, Berkeley.
- Campbell, K.W. and Bozorgnia, Y. (2011), "Prediction equations for the standardized version of cumulative absolute velocity as adapted for use in the shutdown of US nuclear power plants", *Nucl. Eng. Des.*, **241**(7), 2558-2569. <https://doi.org/10.1016/j.nucengdes.2011.04.020>.
- Chávez-Valencia, L.E, Alonso-Guzmán, A., Alonso-Guzmán, E. and Contreras-García, M. (2007), "Modelling of the performance of asphalt pavement using response surface methodology-the kinetics of the aging", *Build. Environm.*, **42**(2), 933-939. <https://doi.org/10.1016/j.buildenv.2005.10.013>.
- Du, W. and Wang, G. (2013), "A simple ground-motion prediction model for cumulative absolute velocity and model validation", *Earthq. Eng. Struct. Dyn.*, **42**(8), 1189-1202. <https://doi.org/10.1002/eqe.2266>.
- Ghanaat, Y., Patev, R. and Chudgar, A. (2015), "Seismic fragility for risk assessment of concrete gravity dams", *Proceeding of the USSD Annual Conference*, Louisville, KY, April.
- Hardy, G., Merz, K., Abrahamson, N.A. and Watson-Lamprey, J. (2006), "Program on technology innovation: Use of cumulative absolute velocity (CAV) in determining effects of small magnitude earthquakes on seismic hazard analyses", EPRI Report MD, 1014099, Palo Alto, CA, and the US Department of Energy, Germantown.
- Hoseini Vaez, S.R. and Arefzade, T. (2017), "Vibration-based damage detection of concrete gravity dam monolith via wavelet transform", *J. Vibroeng.*, **19**(1), 204-213. <https://doi.org/10.21595/jve.2016.17269>.
- Huang, Y.N, Whittaker, A.S. and Luco, N. (2006), "Performance assessment of conventional and base-isolated nuclear power plants for earthquake and blast loading", Technical Report MCEER-08-0019, Department of Civil, Structural and Environmental Engineering, University at Buffalo, State University of New York, USA.
- Hussan, M., Rahman, M.S., Sharmin, F., Kim, D. and Do, J. (2018), "Multiple tuned mass damper for multi-mode vibration reduction of offshore wind turbine under seismic excitation", *Ocean Eng.*, **160**, 449-460. <https://doi.org/10.1016/j.oceaneng.2018.04.041>.
- Ibarra, L.F. and Krawinkler, H. (2005), "Global collapse of frame structures under seismic excitations", Pacific Earthquake Engineering Research Center, Berkeley, CA.
- Ichii, K. (2004), "Fragility curves for gravity-type quay walls based on effective stress analyses", *13th WCEE*, Vancouver, BC, August.
- K-water (2018), Integrated Water Resources Management; Korea Water Resources Corporation, Republic of Korea. http://www.kwater.or.kr/eng/busifacilitiespresentPage.do?s_mid=1190.
- Kartal, M.E., Başıağa, H.B. and Bayraktar, A. (2011), "Probabilistic nonlinear analysis of CFR dams by MCS using response surface method", *Appl. Math. Model.*, **35**(6), 2752-2770. <https://doi.org/10.1016/j.apm.2010.12.003>.
- Katona, T.J. (2013), "Options for the treatment of uncertainty in seismic safety assessment of nuclear power plants", *J. Disast. Res.*, **8**(3), 465-472. <https://doi.org/10.1556/Pollack.5.2010.1.9>.
- Kim, J.H., Choi, I.K. and Park, J.H. (2011), "Uncertainty analysis of system fragility for seismic safety evaluation of NPP", *Nucl. Eng. Des.*, **241**(7), 2570-2579. <https://doi.org/10.1016/j.nucengdes.2011.04.031>.
- Kramer, S.L. and Mitchell, R.A. (2006), "Ground motion intensity measures for liquefaction hazard evaluation", *Earthq. Spectra*, **22**(2), 413-438. <https://doi.org/10.1193/1.2194970>.
- Lee, Y.J. and Lin, C.C. (2003), "Regression of the response surface of laminated composite structures", *Composite Structures*, **62**(1), 91-105. [https://doi.org/10.1016/S0263-8223\(03\)00095-3](https://doi.org/10.1016/S0263-8223(03)00095-3).
- Lin, L. and Adams, J. (2008), "Seismic vulnerability and prioritization ranking of dams in Canada", *Proceedings of the 14th World Conference on Earthquake Engineering*, Beijing, China.
- Mosleh A., Razzaghi, M.S., Jara, J. and Varum, H. (2016), "Development of fragility curves for RC bridges subjected to reverse and strike-slip seismic sources", *Earthq. Struct.*, **11**(3), 517-538. <http://dx.doi.org/10.12989/eas.2016.11.3.517>.
- Mridha, S. and Maity, D. (2014), "Experimental investigation on nonlinear dynamic response of concrete gravity dam-reservoir system", *Eng. Struct.*, **80**, 289-297. <https://doi.org/10.1016/j.engstruct.2014.09.017>.
- Myers, R.H., Montgomery, D.C. and Anderson-Cook, C.M. (2016), *Response Surface Methodology: Process and Product Optimization Using Designed Experiments*, John Wiley & Sons.
- O'Hara, T.F. and Jacobson, J.P. (1991), "Standardization of the cumulative absolute velocity", No. EPRI-TR-100082, Electric Power Research Inst.
- Padgett, J.E. and DesRoches, R. (2008), "Methodology for the development of analytical fragility curves for retrofitted bridges", *Earthq. Eng. Struct. Dyn.*, **37**(8), 1157-1174. <https://doi.org/10.1002/eqe.801>.
- Reed, J.W. and Kassawara, R.P. (1990), "A criterion for determining exceedance of the operating basis earthquake", *Nucl. Eng. Des.*, **123**(2-3), 387-396. [https://doi.org/10.1016/0029-5493\(90\)90259-Z](https://doi.org/10.1016/0029-5493(90)90259-Z).
- Reed, J.W. and Kennedy, R.P. (1994), "Methodology for developing seismic fragilities", TR-103959, Electric Power Research Institute, Palo Alto, California.
- Sadhukhan, B., Mondal, N.K. and Chattoraj, S. (2016), "Optimisation using central composite design (CCD) and the desirability function for sorption of methylene blue from aqueous solution onto Lemna major", *Karbala Int. Journal of Modern Sci.*, **2**(3), 145-155. <https://doi.org/10.1016/j.kijoms.2016.03.005>.
- Sen, U. (2018), "Risk assessment of concrete gravity dams under earthquake loads", Louisiana State University and Agricultural and Mechanical College.
- Tran, T.T., Cao, A.T., Nguyen, T.H.X. and Kim, D. (2019), "Fragility assessment for electric cabinet in nuclear power plant using response surface methodology", *Nucl. Eng. Technol.*, **51**(3), 894-903. <https://doi.org/10.1016/j.net.2018.12.025>.
- Vamvatsikos, D. and Cornell, C.A. (2002), "Incremental dynamic analysis", *Earthq. Eng. Struct. Dyn.*, **31**(3), 491-514. <https://doi.org/10.1002/eqe.141>.
- Wang, J.P., Yun, X., Kuo-Chen, H. and Wu, Y.M. (2018), "CAV site-effect assessment: A case study of Taipei Basin", *Soil Dyn. Earthq. Eng.*, **108**, 142-149. <https://doi.org/10.1016/j.soildyn.2018.02.028>.